Proceedings of the Institute of Acoustics

A SIMPLE 3D MODEL?

C H Harrison

BAeSEMA Ltd, Biwater House, Portsmouth Road, Esher, Surrey. KT10 9SJ

ABSTRACT

One of the most difficult things in underwater acoustics is to see wood for trees. The most straightforward approach is often a computer-intensive numerical solution. Frequently this does not lead to much insight into the physics. This paper discusses some simple underwater propagation models with improving understanding in mind. We start with some simple laws for flat bottoms and range-dependent environments, and rapidly drift into three dimensions. In particular we look at three-dimensional effects with variable bathymetry and describe them with analytical models. These are useful as benchmarks for numerical models and for providing insight into acoustic behaviour. It is often also important to be able to generalise these effects for operational research purposes and system design. Above all we must be able to tell whether the new effects are important, or not, in practice.

1. INTRODUCTION

One might imagine that the advent of extremely powerful 'number crunchers' means the end of all our problems in modelling underwater sound propagation. Although we could have made little progress without them there will always be fundamental dependencies on alternative methods to understand the behaviour of the mechanisms. Often a fully comprehensive correctly run numerical propagation loss plot is no more enlightening than trials data despite the fact that the basic equations for the treatment are obviously known. The alternative, on which we concentrate in this paper, is the construction of analytical formulae. There are several benefits that a simple or analytical approach can provide, and these can be grouped as follows.

Understanding

Analytical formulae are useful for showing the essence of the problem through the dependence of the output on the various inputs. However it is important that the formulae are relatively simple so that dependencies are either explicit or can be easily and quickly evaluated.

Benchmarks

Quite apart from the problem of matching theory with experiment there is the problem of checking that computer-intensive approaches provide correct solutions to the posed mathematical problem. Analytical solutions, whether simple or otherwise, provide useful checks on benchmarks.

A SIMPLE 3D MODEL?

Ockham's Razor

There are several distinct applications for propagation modelling:

- Modelling the physics in its own right
- Providing an input to the design of sonar systems
- Real time predictions.

In all cases there is more to it than just modelling intensity, but the level of complication and detail needs to be commensurate with application. Therefore simplification is justified and, in many cases, necessary.

Significance

A variation on achieving better understanding by using analytical formulae is the ability, in design studies, to check that you are barking up the right tree. It is often easier to see which mechanisms are most important for the application and to make generalisations.

2. GENERAL APPROACHES

2.1 Acoustic Components

A fruitful basis for a simple model is to treat the various acoustic components such as bottom reflection, bottom refraction, Lloyd's mirror, and so on, separately and then add the powers or simply take the largest. This approach has been adopted in the model INSIGHT (Ref 1,2) where full benefit is taken from this extra information. The formulae for each component simplify because they occupy narrower bands of angles where behaviour, whether in deep or shallow water, is more easily predicted. For instance, bottom reflections are steep enough to ignore the water column's velocity profile. The formulae are also selected to reproduce important effects such as slow spatial interference beats (see Fig 1) but to ignore very rapid fluctuations. Because there is only a limited set of angle (or wavenumber) bands it is easy to see that a limited set of component types will cater for all eventualities.

2.2 Variants of 'Mode Stripping'

2.2.1 Range-independent models

In shallow water the dominant loss mechanism is the boundary losses. In normal mode terms each mode spreads cylindrically and decays exponentially, but with faster decay for higher order modes. In ray terms each ray spreads spherically and undergoes one extra boundary loss for each ray cycle. By inserting a grazing angle (θ) dependence on the dB loss per radian per bounce L of

$$L = \alpha\theta \qquad (1)$$

and using a simple law for cycle distance r_c in terms of depth H, e.g.

$$r_c = 2H\cot\theta \qquad (2)$$

one obtains a gaussian dependence of ray intensity on angle over which to integrate. The result if we assume angle limits of zero to effectively infinity is the same using rays or modes and is known as 'mode stripping' (Ref 3). Intensity I is given by

$$I = \varepsilon r^{-3/2} H^{-1/2} \alpha^{-1/2} \tag{3}$$

where

$$\varepsilon = (20\pi/\log_e 10)^{1/2} = 5.22.$$

A numerical demonstration of the associated 15logr law is shown in the comparison with a SAFARI plot for an intermediate depth environment in Fig 2.

There are many possible variants on this theme, all of which result in perfectly viable analytical solutions (Ref 4). One possibility stems from the realisation that all realistic refracting environments will have a non-zero lower angle limit θ_m associated with the largest possible cycle distance. This results in an erfc dependence (see also Ref 31)

$$I = \varepsilon r^{-3/2} H^{-1/2} \alpha^{-1/2} \operatorname{erfc}\left[\theta_m (\alpha r \varepsilon_1/H)^{1/2}\right]$$

$$\text{and } \varepsilon_1 = \left(\log_e 10\right)/20 = \pi/\varepsilon^2 \tag{4}$$

At long range this reverts to

$$I = \varepsilon_1^{-1} r^{-2} \alpha^{-1} \theta_m^{-1} \exp\left[-\theta_m^2 \alpha r \varepsilon_1/H\right] \tag{5}$$

and this can also be seen in Fig 2.

In addition it is possible to deal with single mode propagation (Ref 3), critical angles, boundary loss laws of the form $L = \alpha\theta+\beta$, and linear surface or bottom ducts (Ref 4) where the cycle distance is of the form

$$r_c = 2(c/(dc/dz))\tan\theta. \tag{6}$$

A lesser known variation is apparent from the mode sum derivation. If the source and receiver, at depths z_s, z_r are close to the surface relative to the wavelength λ then the dipole effect associated with the mode shape results in an extra $\sin^4\theta$ in the angle integral. We then have a 35logr law.

$$I = 48 \pi^2 \varepsilon^5 z_s^2 z_r^2 \lambda^{-4} H^{-1/2} r^{-7/2} \alpha^{-5/2} \tag{7}$$

An example of this behaviour is seen in the SAFARI plot in Fig 3. Clearly variations in between 10logr and 35logr are possible.

A SIMPLE 3D MODEL?

2.2.2 Range-dependent models

Finally it is possible to use the same angle integral approach to tackle range dependent media and even 3D effect as we shall see later. The ray invariant

$$\int \frac{\sin\theta}{c}\, dz = \text{constant} \tag{8}$$

where the integral is taken over one complete ray cycle, dictates that ray grazing angles become steeper in shallow water in a reversible fashion provided the environment changes slowly (Ref 5). In an isovelocity medium this simplifies to

$$H\sin\theta = \text{constant} \tag{9}$$

and so the varying θ^2 in the exponent of the original mode stripping integral is still handleable despite the varying depth. The result for a (range-independent) minimum angle θ_m with water depth at source H_s and receiver H_r is

$$I = \pi^{1/2} r^{-1} H_r^{-1} A^{-1/2} \operatorname{erfc}\left[\theta_m A^{1/2}\right] \tag{10}$$

where

$$A = \varepsilon_1 H_s^2 \int_0^r \frac{\alpha\, dr'}{H(r')^3}$$

and the loss law α is allowed to vary with range.

In an isovelocity medium where $\theta_m = 0$ this reduces to a range dependent equivalent of mode stripping (Ref 6).

$$I = \varepsilon (r H_r H_s)^{-1} \left[\int_0^r \frac{\alpha\, dr'}{H(r')^3}\right]^{-1/2} \tag{11}$$

The first term in brackets is simply the geometric spreading effect, and this is offset by the integral that contains all the boundary loss and cycle distance dependence. It turns out that the effect of changing water depth H_r at the receiver can be exactly compensated by boundary losses leaving a net cylindrical spreading if the bottom profile is linear with an upward slope. This inverse problem of calculating the bottom profile responsible for a particular loss law was investigated in Ref 6, but a slightly neater formula with some examples is given in the Appendix.

Another interesting set of cases has the same water depth at the source and receiver ($H_r = H_s$) but variations in between. It is fairly obvious from eq (11) that the intensity will fall slowly for trough-like bathymetry but rapidly for ridge-like bathymetry. These effects have been clearly

demonstrated in some laboratory scale experiments with a 500KHz source and an 'ocean' several centimetres deep (Ref 7). Figure 4 results from a more or less parabolic ridge and Fig 5 results from a parabolic trough levelling out at each end. In both cases an appropriate IFD plot is superimposed. Note that we only reach the point where $H_r = H_s$ at either end of the plot, so the difference caused by the boundary loss alone is evident in comparing the right hand end of Fig 4 with Fig 5. A simple calculation with some example dB losses based on eq (11) are given in the Appendix.

2.3 Empirical Models - 'Trained' Models

There are a number of well known empirical models for shallow water Refs (8-10). These have the obvious advantage that they are based on reality, but on the other hand this 'reality' is only the truth at the time and place of the experiment. For any other conditions, e.g. water depth, bottom loss, sea state, source/receiver depth etc we always rely on some theory to interpolate, or more dangerously, to extrapolate. Typical loss laws are of the form

$$TL = A \log r + Br + C \qquad (12)$$

where the coefficients are frequency dependent (Ref 10).

In between the empirical models and the entirely theoretical is an area with scope for more formal development. One is used to the idea of using a model such as SUPERSNAP (in a regime where it is valid) to explain trials data. Usually one or more parameters need to be 'tweaked' to achieve a match, and given a reasonably large trials database it is possible to convince oneself that systematic corrections to some of the environmental inputs are justified. The separated components type of model that INSIGHT uses is ideal for this because it is much easier to home in on the most suitable parameters to change. Rather than dismissing this approach as just a convenient fudge one could regard it as the equivalent of the training session that is required in applications of neural networks and in this respect is a perfectly valid exercise.

Without going into details one can envisage many techniques with or without humans in the loop for essentially improving the data that goes into models rather than the models themselves. These include optimisation methods such as linear programming in conjunction with a model like INSIGHT to minimise the discrepancy between prediction and experiment by choice of input, regression analysis and even neural networks themselves. The trick is not to expect these methods to out-perform human physicists in anything but mental stamina.

3. EFFECTS IN 3D

In three dimensions the additional effects include refraction out of plane by horizontal velocity gradients due to large scale features such as eddies or small scale features such as internal waves or wakes. Here we restrict ourselves to bathymetric effects where the bending effect can be understood several ways, the simplest being that the bottom slope systematically tilts each reflected ray slightly towards deep water. Since the medium is still nearly stratified one can image local sets of vertical normal modes that have a position-dependent horizontal wave number given by $k^2 - (\pi n/H)^2$ where $k = \omega/c$, H is local water depth and n is mode number. Thus in the horizontal plane

each vertical mode behaves like a ray bending towards regions of high wavenumber as predicted by Snell's law. In addition, of course, one can treat the problem as one of solving the 3D Helmholtz equation, and solutions are possible.

3.1 Ray Paths

By considering the three dimensional geometry of reflected rays it is possible to see that there are two ray invariants (Ref 11), one (seen already in eq 8 and 9) defining ray elevation angle θ in terms of water depth H, the other defining the change in ray azimuth at each bottom reflection. Thus in isovelocity water we have

$$H\sin\theta = \text{constant} \equiv A \tag{13}$$

and for bathymetry with translational symmetry (i.e. depth is a function of y but not x) with ray heading ϕ measured relative to upslope

$$\cos\theta \sin\phi = \text{constant} \equiv B \tag{14}$$

The second invariant is a horizontal equivalent of the Snell invariant $K\sin\phi$ in a stratified medium. Here the horizontal wavenumber K is, from eq 13 with $k=\omega/c$

$$K = k\cos\theta = k\left(1-(A/H)^2\right)^{1/2} \tag{15}$$

This is a constant along the depth contour lines and only varies up or down slope. Consequently eqs (13) and (14) can be used to trace rays in the horizontal plane. In particular there are a number of functional forms of troughs and ridges for which analytical solutions are possible (Ref 11). The simplest of these is the wedge for which ray trajectories are hyperbolic.

In bathymetries with rotational symmetry (i.e. depth is a function of $\rho = (x^2 + y^2)^{1/2}$ only) the second invariant becomes

$$\rho \cos\theta \sin\phi = \text{constant} \tag{16}$$

and analytical solutions are again possible for a conical seamount and the basin defined by

$$H(\rho) = H_o\,(1 + \rho^2/\rho_o^2)^{-1/2} \tag{17}$$

So far there has been no restriction on initial ray angles, but if we intend to follow a particular vertical mode as in Ref 12 the initial elevation angle is fixed through

$$\left(n + \tfrac{1}{2}\right)\lambda = 2\,H \sin\theta \tag{18}$$

Note that because of the ray invariant this remains constant for one mode at all water depths. This is no coincidence. If we had started with the mode number being invariant as required by the adiabatic approximation then the WKB phase integral for that mode, given by

A SIMPLE 3D MODEL?

$$\left(n + \tfrac{1}{2}\right)\pi = \int_{z_B}^{z_T} \left(k^2 - K^2\right)^{1/2} dz \qquad (19)$$

provides another derivation of the ray invariant in eq 8 which reduces to eq (13) and eq (18) for isovelocity water.

Using eq (18) as the definition of the initial elevation angle θ_s corresponding to the nth mode at water depth H_s we can then trace out the rays starting at the arbitrary initial ray headings as in Fig 6. Inevitably, on approaching shallow water, the rays turn towards deep creating the 'fountain' effect seen in Fig 6. The envelope of these curves is clearly a caustic with a shadow on the far side, and behaviour is familiar from the effects of refraction in the vertical plane in range-independent environments.

3.2 Vertical Mode Path in the Horizontal

From a modal point of view there are shadows in the horizontal plane which are a three-dimensional manifestation of the mode cut-off, and it is interesting to calculate their shape. It turns out that analytical solutions are possible for some of the earlier trough, ridge, basin and seamount geometries (Ref 12). One example is the wedge (Fig 7) where the envelopes are again hyperbolae. However, as will be discussed later, it must be remembered that these shapes are for loss-free bottoms, and introducing bottom losses can make important differences particularly in the upslope direction. Nevertheless, whether dominated by geometric effects or losses the onset of mode cut-off generally occurs earlier (i.e. in deeper water) than one would expect if thinking in terms of the vertical plane joining source and receiver.

3.3 Ray/Mode Intensity

There are many ways of tackling intensity in three-dimensions. These include solving the wave equation analytically for the wedge (Ref 13) and evaluating the resulting integral with the stationary phase method (Ref 14), reducing the wave equation to vertical modes with a horizontal eikonal equation (Ref 15), using the adiabatic approximation (Ref 16), using the WKB approximation in the horizontal plane (Refs 17, 18) and the 3D parabolic equation (Ref 19). The horizontal ray behaviour means that it is possible to use straightfoward flux arguments to construct an intensity for each mode using ray invariants (Ref 17). This is most simply a depth-averaged intensity akin to the adiabatic incoherent mode sum. It is also possible to calculate an intensity taking phase into account by considering rays with phase. Harrison showed in Ref (17) that Buckingham's solution for a wedge can be reproduced by this method.

By considering adjacent rays separated initially by $d\theta_s$ in elevation angle and $d\phi_s$ in azimuth we can write a relative intensity I (such that transmission loss TL = -10logI) as

$$I = 2 \int_0^{\theta_s} \left|\frac{d\phi_s}{dy}\right| \frac{d\,\theta_s \cos\theta_s}{H \sin\phi \cos\theta} \qquad (20)$$

A SIMPLE 3D MODEL?

Here θ_l is a limiting angle at the source where the elevation angle is θ_s, and other subscript-less variables are at the receiver. No particular geometry is implied provided y is the local upslope direction and ϕ is measured relative to y. This equation can be turned into the equivalent of an incoherent mode sum by substituting the differential of eq (18) at the source

$$\frac{dn}{d\theta_s} = 2 H_s \cos\theta_s/\lambda \tag{21}$$

giving

$$1 = \sum_{n=1}^{N} \left|\frac{d\phi_s}{dy}\right| \frac{\lambda}{H H_s \sin\phi \cos\theta} \tag{22}$$

Whether this formula's solution can be made explicit now depends on whether $d\phi_s/dy$ and $\sin\phi$ can be evaluated at the receiver.

For a wedge with x along the wedge axis and y pointing horizontally to deep water the ray equations relating x, y to x_s, y_s and θ_s, ϕ_s are known (Ref 12), and one can separate out $d\phi_s/dy$ to give an intensity for the nth mode of

$$I_n = \frac{\lambda\, y \sin\phi_s}{H H_s\, x\, (x \sec^2\theta_s \cot\phi_s - y_s)\cos\theta_s} \tag{23}$$

One can also eliminate ϕ_s, which typically has two values, one for the more or less direct path, the other for the horizontally 'reflected' path (akin to horizontal Lloyd's mirror, see Ref 18), and the result is

$$I_n = \frac{\lambda}{H H_s} \frac{y}{d\cos\theta_s} \left(\frac{1}{s_+} + \frac{1}{s_-}\right) \tag{24}$$

Here

$$d = \left(y^2 - y_s^2 \sin^2\theta_s - x^2 \tan^2\theta_s\right)^{1/2} \tag{25}$$

is a 'Pythagorean' distance from the caustic or shadow boundary (since d=0 is the equation for the caustic from Ref 12), and s_+, s_- are the total ray lengths for the two paths. A theorem from Ref 11 shows that

$$s_\pm = x \sec\theta_s \operatorname{cosec}\phi_s^{\,x} \tag{26}$$

or eliminating ϕ_s

$$s_\pm^2 = y_s^2 \cos^2\theta_s + x^2 \sec^2\theta_s + d^2 \pm 2 y_s\, d \cos\theta_s \tag{27}$$

Equation (27) combined with eq (24) completely defines the intensity in terms of initial angle θ_s or mode number n. As one would expect +/- values converge at the caustic when d=0. In addition one has the usual problem with ray formulae at caustics (d=0) that the intensity tends to infinity.

Despite this it is shown in Ref (17) that eq (24) is identical with the spatially averaged modulus square of Buckingham's first order stationary phase solution (eq 24 of Ref 14) which is valid away from the caustic. In the vicinity of the caustic Buckingham's approach requires a second order stationary phase solution although one might guess by analogy with the study of caustics in refracting media that there would be an Airy function dependence at right angles to the caustic. This is explored in conjunction with the associated horizontal WKB solutions in Ref (18).

3.4 Boundary Losses

Equation (24) like the equivalent wave solutions gives a loss-free intensity, and away from the caustic where y - d the only difference between it and the adiabatic incoherent mode sum is the distinction between straight horizontal range and the two ray lengths $s_{\pm}$. This implies that apart from interference effects and the shadow the only major three dimensional geometric effects that any wave solution can produce is the dependence on water depth H! With lossy boundaries, of course, the story is different, but then three-dimensional effects have less time to develop before all rays are lost.

The essence of the bottom loss problem is incorporated in eq (11), but there are some subtle differences in three dimensions (Ref 20). When there is a critical angle θ_c the ray invariant (eq 13) shows that for a given initial elevation angle the point where that angle is reached is the contour line for depth H_c where

$$H_c = H_s \sin\theta_s / \sin\theta_c \tag{28}$$

For instance, in Fig 6 the effect is simply to truncate all rays that attempt to pass H_c into shallower water. In effect, only rays that undergo relatively small azimuth changes survive. In addition the caustic structure is eliminated in the shallow water and can only exist for depths greater than H_c (at the side in Fig 6).

Reference 20 shows that the cumulative bottom loss L (equivalent to the integral in eq 11) can be calculated for loss per bounce R proportional to sinθ

$$R(\theta) = \alpha \sin\theta \tag{29}$$

$$L = \int \frac{\alpha \sin^2\theta \, dy}{2 H \cos\phi} \tag{30}$$

Using the ray invariants this can be evaluated for several cases. One is a ray travelling upslope from the source and back out to infinity in a wedge of angle γ, where

$$L = \frac{\alpha}{2\gamma}\left[\cos\theta_s \cos\phi_s + \left(1 - \cos^2\theta_s \sin^2\phi_s\right)^{1/2}\right] \tag{31}$$

A parameterised version of this function is shown in Fig 8. Clearly the heaviest losses are for initially low grazing angles travelling directly upslope. For example, putting α = 1dB/radian and

A SIMPLE 3D MODEL?

a bottom slope of 1 in 50 (1°) gives 50dB under these conditions or 25dB for $\phi_s = 60°$ (a bistatic angle of 120°). In practice this loss will be very much understated because the linear loss assumption means that even at a grazing angle of 90° where the upslope ray turns round and heads downslope the loss per bounce is only α, i.e. 1dB in the case! If the linear law operates up to a critical angle then rays can only survive by, at worst, grazing the critical depth contour. At this point $\phi = 90°$, and the second ray invariant (eq 14) provides a lower limit on ϕ_s (below which losses are infinite) of

$$\sin\phi_s = \cos\theta_c/\cos\theta_s \tag{32}$$

Thus if the critical angle were 30° with initial elevation angle close to zero, the minimum angle ϕ_s relative to upslope would be 60°.

3.5 Wave Solutions

Analytical wave solutions for the loss-free wedge and conical seamount are well known (Refs 13, 14 and 21). There are also some solutions taking losses into account (Refs 22, 23). Taking the loss-free wedge case the Helmholtz equation is written in polar coordinates (x along the wedge axis, r orthogonal to it and polar angle θ, not to be confused with ray angles) with a source at $(0, \theta_s, r_s)$ and wavenumber $k = \omega/c$ as

$$\frac{\partial^2 \psi}{\theta\, r^2} + \frac{1}{r}\frac{\partial \psi}{\partial r} + \frac{1}{r^2}\frac{\partial^2 \psi}{\partial \theta^2} + \frac{\partial^2 \psi}{\partial x^2} + k^2 \psi = -\frac{2}{r}\delta(r - r_s)\,\delta(x)\,\delta(\theta - \theta_s) \tag{33}$$

This is solved by taking a sine transform in θ, a Hankel transform in r and a Laplace (or Fourier) transform in x. The result for a wedge of angle γ is

$$\psi = \frac{4\pi}{\gamma}\sum_{n=0} \sin(m\,\theta_s)\sin(m\,\theta)\,I_m \tag{34}$$

and

$$I_m = \int_0^\infty J_m(Kr_s)\,J_m(Kr)\,K\,\frac{e^{-px}}{p}\,dk \tag{35}$$

where

$$p = (K^2 - k^2)^{1/2} \tag{36}$$

$$m = n\,\pi/\gamma \tag{37}$$

with n being an integer for pressure release boundaries.

Here K is a dummy variable corresponding to wavenumber in the vertical r, θ plane. Because the integrand of I_m is highly oscillatory it is only possible to make further progress analytically by employing such techniques as stationary phase. As we have shown above there is much more insight to be gained from the simpler ray invariant or adiabatic approach (eq 24), and an incoherent version of eq (34) is identical to it.

A SIMPLE 3D MODEL?

A new approach yielding 'nearly exact' solutions in many more bathymetries with translational symmetry is explored in Ref (18). Although the results are similar to those given by the adiabatic approximation, where one would simply insert a position dependent wavenumber, as in eq (15), into a horizontal two-dimensional Helmholtz equation, the adiabatic approximation is not invoked in this treatment. Instead the environment is transformed into a flat bottomed one where *normalised depth* ζ is the vertical coordinate rather than physical depth z (see Fig 9). This is similar to the 'wedge mode' idea in Ref 24. The Cartesian x, y, z coordinate system is replaced by the orthogonal system ξ, η, ζ with η running along the 'flow lines' in Fig 9 and ζ running at right angles to them. The water depth $h(\eta)$ is also measured along the curved line. The Helmholtz equation becomes

$$\frac{1}{h^2}\frac{\partial^2\psi}{\partial\xi^2} - \frac{h''}{h}\zeta\frac{\partial\psi}{\partial\zeta} + \frac{\partial^2\psi}{\partial\eta^2} + \frac{h'}{h}\frac{\partial\psi}{\partial\eta} + \frac{\partial^2\psi}{\partial\xi^2} + k^2\psi = -\frac{4\pi}{h}\delta(\zeta-\zeta_s)\,\delta(\eta-\eta_s)\,\delta(\xi) \tag{38}$$

where dashes represent differentiation with respect to η.

For the special case of a wedge with $h=\gamma\eta$ we find that this equation reduces to the polar coordinates of eq (33) ($\xi\rightarrow x$, $\eta\rightarrow r$, $\zeta\rightarrow\theta/\gamma$). Generally, if we neglect bottom curvature h" a number of new solutions are possible by carrying out a sine transform in ζ, a Fourier transform in ξ and a modified transform in η. We find that there are two classes of solution, those that are bounded on both sides in η (i.e. 'troughs'), and those that are either unbound or bounded on one side only (i.e. 'ridges').

The former trough equations are described by a double sum of modes in the vertical (index n) and horizontal (index j).

$$\psi = \sum_n b_n \sum_j \frac{u_j(\eta_s)\,u_j(\eta_r)}{K_j}\,e^{iK_j\xi} \tag{39}$$

where

$$b_n = 4\pi i \sin(\nu_n\zeta_s)\sin(\nu_n\zeta_r) \tag{40}$$

$$\nu_n = n\pi \tag{41}$$

and the u_j represent a discrete set of horizontal eigenfunctions with eigenvalues K_j of the equation

$$\frac{\partial^2 u_j}{\partial\eta^2} + \frac{h'}{h}\frac{\partial u_j}{\partial\eta} + \left(k^2 - \frac{\nu_n^2}{h^2} - K_j^2\right)u_j = 0 \tag{42}$$

In the case of ridges there is a similar equation except that the sum over j becomes an integral over a continuous spectrum of modes.

Interestingly, solutions are possible for most of the profiles that provided ray trajectories through use of ray invariants. The troughs include:

A SIMPLE 3D MODEL?

1) 'Lorentz': $h(\eta) = h_o/(1+\eta^2/r_o^2)^{1/2}$
This reduces eq (42) to the 'simple harmonic oscillator' with a solution in terms of Hermite polynomials.

2) The ellipse: $h(\eta) = h_o\,(1-\eta^2/r_o^2)^{1/2}$
Solution are in terms of Mathieu functions.

3) 'Epstein' $h^{-2}(\eta) = -A\ \mathrm{sech}^2\ (\eta/r_o) + B\ \tanh\ (\eta/r_o) + C$
Solutions are in terms of Jacobi polynomials

The ridges include:

1) The wedge: $h(\eta) = \gamma\eta$
The solution is in terms of mth order Bessel functions and is identical to eq (35)

2) 'Curved shelf': $h^{-2}(\eta) = A\eta + B$
The solution is in terms of Airy functions

3) 'Inverse parabolic': $h = h_o/(1 - \eta^2/r_o^2)^{1/2}$
Behaviour is analogous to that at a velocity maximum in a range-independent refracting medium, and the solution is in terms of parabolic cylinder functions.

4) 'Hyperbolic': $h = h_o\,(1 + \eta^2/r_o^2)^{1/2}$
The solution is in terms of modified Mathieu functions.

In addition one can transform eq (42) to

$$\frac{d^2 u_j}{d\eta^2} + \left(K_\eta^2 - \frac{\nu_n^2}{h^2} + \varepsilon\right)u_j = 0 \qquad (43)$$

where ε is small, possibly negligible,

$$\varepsilon = \frac{1}{4}\frac{h'^2}{h^2} - \frac{1}{2}\frac{h''}{h} \qquad (44)$$

and

$$K_\eta^2 = k^2 - K_j^2 \qquad (45)$$

This has yet a new set of solutions. We can employ the WKB solution (and for that matter, an Airy function near to horizontal caustics)

$$u_j(\eta) = \sin\left[\int^\eta \left(K_\eta^2 - \frac{\nu_n^2}{h^2} + \varepsilon\right)^{1/2} d\eta + \pi/4\right]\left(K_\eta^2 - \frac{\nu_n^2}{h^2} + \varepsilon\right)^{-1/4} N^{-1/2} \qquad (46)$$

where N is a normalisation constant. The 3D solution for a WKB trough is

$$\psi = \sum_n \sum_j b_n \frac{u_j(\eta_s)\, u_j(\eta_r)\, e^{iK_j\xi}}{K_j (h(\eta_s)\, h(\eta_r))^{1/2}} \tag{47}$$

The discrete mode eigenvalues are given by the 'phase integral'

$$\left(j + \tfrac{1}{2}\right)\pi = \int \left(K_\eta^2 - \frac{\nu_n^2}{h^2} + \varepsilon\right)^{1/2} d\eta \tag{48}$$

where the integral is taken between points where the integrand is zero.

4. EXPERIMENTS

4.1 Questions

There are a number of questions on real life 3D propagation that have not been convincingly answered yet. Amongst these are

1) Are there significant out of plane effects as far as intensity is concerned?
2) Are there significant out of plane effects as far as angle, coherence and delay time are concerned?
3) Under what conditions is the adiabatic approximation valid in a refracting environment?

The final answer will come from at sea experiments, however these are notoriously difficult to do (Ref 25), partly because to be convincing, they need angle measurements at the source and receiver end. This helps to distinguish between the multiple reflection turning mechanism and other mechanisms such as bottom scattering which may be more effective at smaller bistatic angles.

It is easier to perform controlled experiments in laboratory conditions. Glegg et al (Ref 26) have performed experiments at several kHz in a swimming pool size tank. Some experiments with a more faithful aspect ratio have been performed by Lian Sheng Wang (Ref 27-28) at 500KHz with a one centimetre deep, two metre square 'ocean' above a fine sand bottom. It has been possible to investigate propagation in a wedge and various troughs and ridges (Ref 7). By separating modes and monitoring their evolution one can investigate criteria for the applicability of the adiabatic approximation (Ref 29). Nevertheless these experiments are all done with isovelocity water and the problem of adiabatic applicability is more difficult with range-dependent sound speed. The transformation method of Section 3.5 suggests that the adiabatic approximation is only 100% valid when the new coordinate system is separable. Thus one might expect the adiabatic approximation to be sufficient for a V-shaped channel provided it only varied with range in width or velocity contrast, but one would not expect splitting into more than one duct to be accommodated. In practice, of course, there may be cases where the adiabatic approximation happens to be a reasonable compromise despite drastic changes in the profile.

4.2 A Proposal

Another way of looking at the question of the importance of three-dimensional effects is that if one cannot devise an experiment that is sufficiently accurate to prove that the effect exists then it is probably pointless worrying about the effect.

Harrison (Ref 30) proposed an experiment designed to prove conclusively that these effects are significant. He made the point that there were at least two mechanisms that one might find at the edge of an ocean basin which could give similar azimuthal dependence. One was the multiple reflection mechanism discussed above, and the other was the backscattering from the basin edge identified with large shot sources.

With a large bistatic angle Φ the ray elevation angles will not exceed $(\pi-\Phi)/2$, so if the seabed is smooth, backscattering will be weak and multiple reflection will be as important as modal propagation ever is. On the other hand with a small bistatic angle and a rough seabed the multiple reflection mechanism will be wiped out leaving backscattering. Therefore each mechanism must at least be dominant in some circumstances.

This suggests that a promising experimental approach is to stick to large bistatic angles, virtually across slope propagation, and to search for modal shadow zone boundaries, in particular the first mode cut-off and the transition from single mode to two modes. A plan view is shown in Fig 10. The idea is to place a vertical array near the slope and to use it to separate out modal arrivals from a source which maps out the region as shown.

Although the shadow pattern is shown here as fixed, it should be remembered that the shadow boundaries all move in towards the shore line as frequency is raised. Therefore a sweep in frequency is as good as a spatial sweep. Multiple or single tone sources or shots could be used. The main distinction between multiple bottom reflection and scattering is that the spatial pattern exists in the former mechanism but not the latter. However, sea surface roughness will provide an important tool for distinction since increasing roughness will enhance scattered returns but weaken multiple reflection paths.

The dependence on bistatic angle is automatically included in the experiment by mapping out the intensity. It is most likely that the multiple reflection mechanism will dominate towards the right (large bistatic angles) whereas the scattering mechanism will dominate towards the left (small bistatic angles).

5. CONCLUSIONS

We have looked at the virtues of simple propagation models (including empirical ones) in various applications and cited some useful examples for range-independent, through range-dependent to three dimensional models.

The additional effects of the third dimension were reviewed starting with a ray invariant approach. This included geometric spreading and boundary losses.

A SIMPLE 3D MODEL?

With the emphasis more on analytical than simple we briefly visited various wave solutions to the three dimensional Helmholtz equation and listed geometries other than the wedge for which solutions are possible.

Finally we looked at 3D laboratory and sea trial work, and proposed a trial to demonstrate the existence of modal shadows in a real ocean environment and thereby prove the importance of 3D effects.

ACKNOWLEDGEMENT

The work attributed here to the author was supported largely as private venture work by BAeSEMA although the original ray invariant work was done whilst on exchange at Naval Research Laboratory, Washington DC. BAeSEMA also contributed support to the collaborative experimental work with Dr Nick Pace and Lian Sheng Wang of Bath University. Finally I am indebted to the UK MoD for the notion of a 'simple model' which was inspired by contract work for what is now the Defence Research Agency.

REFERENCES

[1] C H Harrison, M A Ainslie, M N Packman "INSIGHT: A fast, robust propagation loss model providing clear understanding", UDT Conference Proceedings Feb (1990).

[2] C H Harrison, "From advanced to simple propagation models", Proc Institute of Acoustics, 12 Part 2, 13-28, (1990).

[3] D E Weston, "Intensity-range relations in oceanographic acoustics", J Sound and Vibration 18, 271-287, (1971).

[4] C H Harrison, "Simple formulae for ducts", YARD Technical Report M540/TR/2, September (1990).

[5] D E Weston, "Guided propagation in a slowly varying medium", Proc Phys Soc 73, 365-384, (1959).

[6] D E Weston, "Propagation in water with uniform sound velocity but variable-depth lossy bottom", J Sound and Vibration 47, 473-483, (1976).

[7] M A Ainslie, N G Pace, Lian Sheng Wang, C H Harrison, "Numerical and laboratory modelling of propagation over troughs and ridges", in preparation.

[8] H W Marsh, M Schulkin, "Shallow water transmission", J Acoust Soc Am, 34, 863 (1962).

[9] P H Lindop, "The deduction of approximate values of sediment depth from propagation loss measurements", in 'Ocean Seismo-Acoustics', ed T Akal & J M Berkson, NATO Conference Series IV, Vol 16, (1985).

A SIMPLE 3D MODEL?

[10] O F Hastrup, "Acoustic experiments in the South Western Approaches to the English Channel", SACLANT Report SR-72, [C], (1983).

[11] C H Harrison, "Three-dimensional ray paths in basins, troughs and near seamounts by use of ray invariants", J Acoust. Soc. Am. 62, 1382-1388, (1977).

[12] C H Harrison, "Acoustic shadow zones in the horizontal plane", J Acoust. Soc. Am. 65, 56-61, (1979).

[13] M J Buckingham, "Acoustic propagation in a wedge-shaped ocean", in 'Acoustics and the Sea-bed', ed N G Pace, Proc Inst Acoust, Bath University Press, (1983).

[14] M J Buckingham, "Theory of acoustic radiation in corners with homogeneous and mixed perfectly reflecting boundaries", J Acoust Soc Am, 86, 2273-2291, (1989).

[15] H Weinberg and R Burridge, "Horizontal ray theory for ocean acoustics", J Acoust. Soc Am, 55, 63-79, (1974).

[16] M Porter, "The KRAKEN normal mode program", SACLANT Memorandum SM-245, (1991).

[17] C H Harrison, "An analytic intensity in a wedge-shaped ocean", in Proceedings of '3rd IMACS Symposium on Computational Acoustics', June 1991, ed D Lee (1993) in press.

[18] C H Harrison, "Wave solutions in three dimensional ocean environments", J Acoust Soc Am, (1993) in press.

[19] D Lee, G Botseas and W L Siegmann "Examination of three-dimensional effects using a propagation model with azimuth - coupling capability (FOR3D), J Acoust Soc Am, 91, 3192-3202, (1992).

[20] C H Harrison, "Ray/mode trajectories and shadows in the horizontal plane by ray invariants", in 'Hybrid formulation of wave propagation and scattering' ed L B Felsen, NATO ASI No. 86, Martinus Nijhoff, Dordrecht (1984).

[21] M J Buckingham, "Theory of acoustic propagation around a conical seamount", J Acoust Soc Am, 80, 265-277, (1986).

[22] M J Buckingham, "Theory of three dimensional acoustic propagation in a wedge-like ocean with a penetrable bottom", J Acoust Soc Am 82, 198-210, (1987).

[23] G B Deane and C T Tindle, "A three-dimensional analysis of acoustic propagation in a penetrable wedge slice", J Acoust Soc Am 92, 1583-1592, (1992).

[24] H Primack and K E Gilbert, "A two-dimensional downslope propagation model based on coupled wedge modes", J Acoust. Soc. Am. 90, 3254-3262, (1991).

[25] R Doolittle, A Tolstoy and M J Buckingham, "Experimental confirmation of horizontal refraction of C W acoustic radiation from a point source in a wedge-shaped ocean environment", J Acoust. Soc Am, 83, 2117-2125, (1988).

[26] S A L Glegg, A Hundley, J M Riley, J Yuan and H Uberall, "Laboratory scale measurements and numerical predictions of underwater sound propagation over a sediment layer", J Acoust Soc Am 92, 1624-1630, (1992).

[27] L S Wang, N G Pace, M A Ainslie, C H Harrison, "Experimental study of sound propagation in modelled shallow water environments, submitted to Ultrasonics.

[28] L S Wang, N G Pace, C H Harrison, M A Ainslie, "Sound propagation in wedge-shaped ocean channels", in preparation.

[29] C H Harrison, L S Wang, N G Pace, M A Ainslie, "An experimental investigation of mode coupling", in preparation.

[30] C H Harrison, "Scattering in basins or horizontally refracting modes: which is it?", J Acoust Soc Am, S1, 82, (1987).

[31] J D MacPherson, M J Daintith, "Practical model of shallow water acoustic propagation", J. Acoust. Soc. Am, 41, 850-857 (1967).

APPENDIX : EVALUATIONS OF THE SIMPLE RANGE-DEPENDENT MODEL

A.1 Evaluation of Intensity

Starting with eq (11) in the main text we evaluate the intensity in the vicinity of symmetrical ridges and troughs of the form

$$\frac{1}{H(r)^3} = A + B\,\mathrm{sech}^2((r - r_m)/w) \tag{A1}$$

with $A > 0$, $A + B > 0$. The feature has half width w and is centred at range r_m, some way from the source. Thus the water depth at the source is

$$\frac{1}{H_s^3} = A + B\,\mathrm{sech}^2(r_m/w) \approx A \tag{A2}$$

and the maximum or minimum depth is given by

$$\frac{1}{H_m^3} = A + B \tag{A3}$$

A SIMPLE 3D MODEL?

A trough therefore has negative B whereas a ridge has positive B.

Equation (11) becomes

$$I = \frac{\varepsilon\,([A + B\,\mathrm{sech}^2(r_m/w)]\,[A + B\,\mathrm{sech}^2((r - r_m)/w)])^{1/3}}{\alpha^{1/2}\,r\,\{Ar + wB\,[(\tanh(r_m/w) + \tanh((r - r_m)/w))]\}^{1/2}} \quad \text{(A4)}$$

When H_r is on the far side of the ridge or trough at $r=2r_m$ we have

$$I = \varepsilon\, r^{-3/2}\, H_s^{-1/2}\, \alpha^{-1/2}\, g \quad \text{(A5)}$$

where g is the factor by which this differs from flat-bottomed mode stripping (cf eq (3)), given by

$$g = \left\{\left[1 - \left(\frac{H_s^3}{H_m^3} - 1\right)\mathrm{cosech}^2(r/2w)\right] + \left(\frac{2w}{r}\right)\left(\frac{H_s^3}{H_m^3} - 1\right)\coth(r/2w)\right\}^{-1/2} \quad \text{(A6)}$$

This simplifies for narrow ridges and troughs $2w \leq r$ to

$$g = \left\{1 + (2w/r)\left(\frac{H_s^3}{H_m^3} - 1\right)\right\}^{-1/2} \quad \text{(A7)}$$

The corresponding increase in loss $\Delta L = -10 \log_{10} g$ is tabulated in Table A1.

Table A1 : Extra loss ΔL for extremum depth H_m relative to depth at source H_s

2w/r	H_m/H_s	ΔL(dB)
.5	.25	7.56
.5	.5	3.26
.5	1	0
.5	1.5	-.94
.5	2	-1.25
.5	4	-1.47
1.0	.25	7.91
1.0	.5	3.55
1.0	1	0
1.0	1.5	-1.16
1.0	2	-1.57
1.0	4	-1.88

A SIMPLE 3D MODEL?

If the extremum depth H_m is between 0.5 and 1.5 H_s the effects are quite small. There are more dramatic losses in the ridge case if rays reach the critical angle, as may be the case in Fig 4. This, of course, would violate the assumption of linear bottom loss angle dependence, but the ray invariant analysis can still be followed through with a higher power law such as $\alpha\theta^n$.

A2 Calculation of the Bottom Profile given the Loss Law

It is possible to go slightly further than Ref 6 to obtain an explicit relation for the depth profile H(r) in terms of the loss law I(r). Starting from eq (11) for clarity we extract the range dependent part F(r)

$$F^2 = \left[r^2 H_r^2 \int_0^r \frac{dr}{H^3} \right]^{-1} \tag{A8}$$

where

$$I = \varepsilon H_s^{-1} \alpha^{-1/2} F \tag{A9}$$

After rearranging and differentiating with respect to r this becomes

$$\frac{1}{H^3} = \frac{d}{dr}\left(\frac{1}{F^2 r^2 H^2} \right) \tag{A10}$$

Defining a new variable

$$J = Fr\, H \tag{A11}$$

this can be written as

$$\left(\frac{Fr}{J} \right)^3 = \frac{d}{dr}\left(\frac{1}{J^2} \right) \tag{A12}$$

$$= \frac{dJ}{dr}\left(\frac{-2}{J^3} \right)$$

$$\frac{dJ}{dr} = -\frac{1}{2}(Fr)^3 \tag{A13}$$

If the desired law F(r) is to be obeyed from some range r_o out to r then integration of eq (A13) gives

$$J(r) - J(r_o) = -\frac{1}{2}\int_{r_o}^{r} (Fr)^3\, dr \tag{A14}$$

which on substitution of eq (A11) gives an explicit formula for H(r) (for $r > r_o$) in terms of F(r)

$$H(r) = \frac{F(r_o)\,H(r_o)\,r_o \; - \; \frac{1}{2}\int_{r_o}^{r} (Fr)^3\,dr}{F(r)\,r} \qquad \text{(A15)}$$

Some examples, including those of Ref 6, are given in Table A2. All clearly reduce to H_o (i.e. $H(r_o)$) at $r = r_o$. The third example reduces to the usual flat bottom mode stripping formula if $a^2 = H_o = H_o$ (cf eq (A9) and eq (3)), but the formula shows that the same law can also be obtained for other profiles.

Table A2 : Example profiles H(r) for given loss laws F(r)

F(r)	H(r)
a/r	$H_o - a^2(r - r_o)/2$
a/r^2	$H_o\,(r/r_o) - a^2\left(r^2 - r_o^{\,2}\right)/4r\,r_o^{\,2}$
$a/r^{3/2}$	$a^2 + \left(H_o - a^2\right)\,(r/r_o)^{1/2}$
a	$H_o\,(r_o/r) \; - \; a^2\left(r^4 - r_o^{\,4}\right)/8r$
ae^{-br}/r	$H_o\,e^{b(r - r_o)} - a^2\,e^{-2br}\left(e^{3b(r - r_o)} - 1\right)/6b$
a/r^{n+1}	$H_o\,(r/r_o)^n - a^2\,r^n\left(r_o^{\,-3n+1} - r^{-3n+1}\right)/2(3n - 1)$ for $n \neq 1/3$
$a/r^{1/3}$	$H_o\,(r/r_o)^{1/3} - \left(a^2 r^{1/3}/2\right)\,\ln\,(r/r_o)$

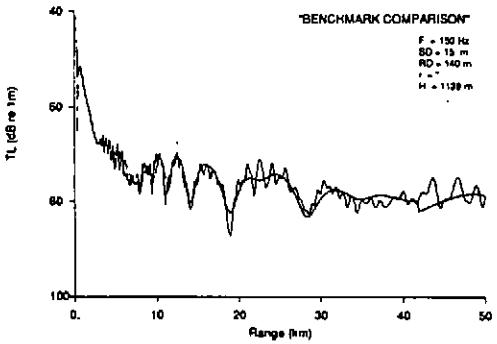

Fig 1 A comparison of the simple model INSIGHT with a rigorous treatment, SAFARI.

A SIMPLE 3D MODEL?

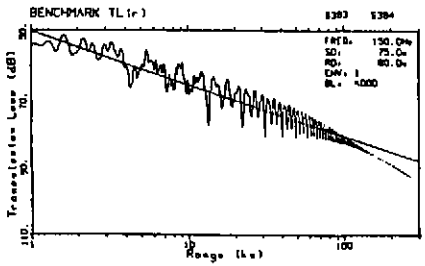

Fig 2 An example of 15 log r dependence ('mode stripping') from SAFARI.

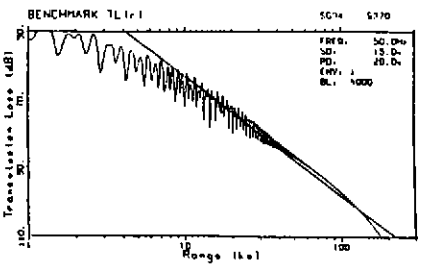

Fig 3 An example of 35 log r dependence from SAFARI.

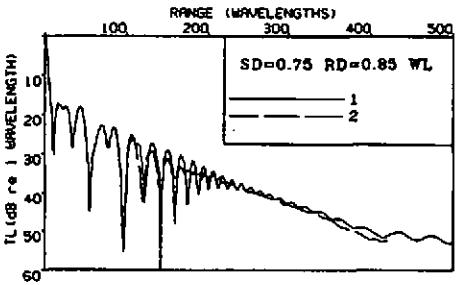

Fig 4 The effect of crossing a ridge. Laboratory experiment at 500kHz (dashed line) compared with IFD (solid line).

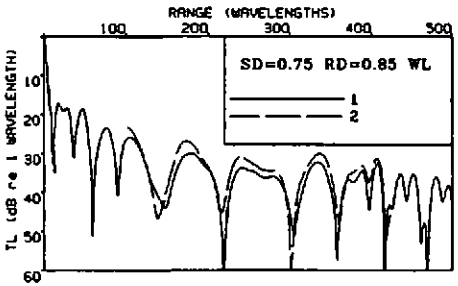

Fig 5 The effect of crossing a trough. Laboratory experiment at 500kHz (dashed line) compared with IFD (solid line).

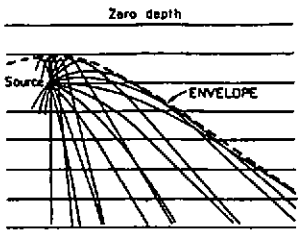

Fig 6 Vertical normal modes behave as horizontal rays. One mode provides a 'fountain' of rays bounded by an envelope.

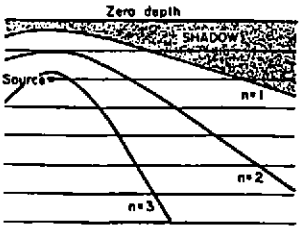

Fig 7 Each mode has a shadow in the horizontal plane. The boundary is defined by the envelope in Fig 6. Closest to the shore line is the complete shadow that is the equivalent of the first mode cut-off in 3D.

A SIMPLE 3D MODEL?

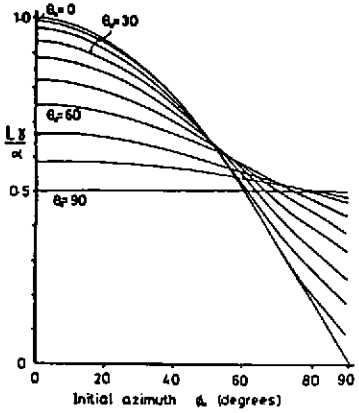

Fig 8 Dimensionless loss versus initial azimuth ϕ_0 for a ray (or mode) travelling up-slope from the source and back out to infinity. L = Total Loss (dB); α = Bottom Loss (dB/radian); γ = Bottom slope (radian).

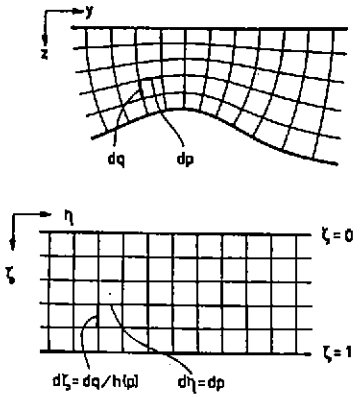

Fig 9 A coordinate transformation. (a) Real space showing the Cartesian coordinates y, z and the relation between them and the curvilinear coordinates p, q. (b) Mapped space showing vertical lines of constant p and horizontal lines of constant q. The final mapped system is η, ζ with ζ being dimensionless (normalised depth).

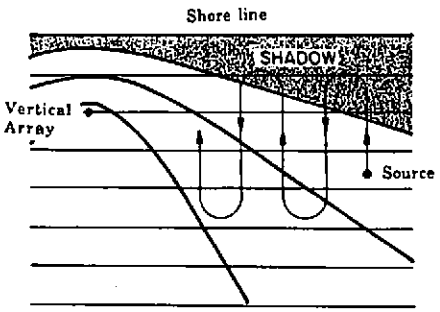

Fig 10 An at-sea experimental arrangement for demonstrating the significance of 3D effects.